

COLLIMATOR SCAN BASED BEAM HALO MEASUREMENTS IN LHC AND HL-LHC*

P. Hermes[†], M. Giovannozzi, C. E. Montanari¹, S. Morales Vigo^{2,3}, M. Rakic⁴, S. Redaelli,
B. Salvachua, CERN, Geneva, Switzerland, ¹also at University of Manchester, UK,
²also at Cockcroft Inst. Accel. Sci. Tech., Warrington, Cheshire, UK,
³also at University of Liverpool, UK, ⁴also at EPFL, Lausanne, Switzerland

Abstract

Measurements in the CERN Large Hadron Collider (LHC) have indicated that the population of the transverse beam halos is greater than that of a Gaussian distribution. With the upcoming High-Luminosity project (HL-LHC), the stored beam energy in the beam halo could become large enough to threaten the integrity of the collimation system. Given the unprecedented stored beam energies of about 400 MJ, currently achieved at the LHC, and roughly 700 MJ planned at the HL-LHC, conventional measurements are difficult. Considerable efforts in the ongoing LHC Run 3 are dedicated to characterising experimentally the transverse beam halos, and its diffusion properties, after the LHC Injector Upgrade (LIU) in preparation for HL-LHC operation. Halo and diffusion measurements are currently based on collimator scans, where robust collimators are inserted in steps into the circulating beam halo. In this contribution, we present techniques for halo characterisation employed in LHC and compare results obtained from such measurements in LHC Run 2 and the ongoing LHC Run 3. We present plans for measurements in the remainder of LHC Run 3 and describe the expected challenges for halo characterization in HL-LHC.

INTRODUCTION

The Large Hadron Collider (LHC) at CERN is a 27 km long circular collider for protons and heavy ions [1]. LHC design beam intensities are so high that even small amounts of beam loss can generate beam dumps, triggered by the interlock system, magnet quenches, or even damage to machine equipment. To preserve the integrity of the machine hardware and avert potential hazards arising from uncontrolled beam losses, the LHC is equipped with a multi-stage collimation system, predominantly located in the betatron collimation insertion region IR7 [1, 2]. Additional details on the collimation system are provided in the following section.

While methods of active and non-destructive monitoring of beam halos are currently under study [3], the current state-of-the-art method for studying the beam halo is scraping with the LHC collimators. In LHC Run 1 (2009–2013) and Run 2 (2015–2018) measurements, up to 5% of the total stored beam energy was found at transverse amplitudes greater than $3\sigma_N$ [4] in a given transverse plane (we refer to this subset of beam particles as *halo* in the following). σ_N denotes the nominal beam size using the LHC's nominal

normalised emittance of $3.5\mu\text{m rad}$. Measured emittances were typically smaller than this conservative value. With the upcoming High Luminosity upgrade (HL-LHC) [5], stored beam energies in the order of 700 MJ are expected to be reached. The scaling to different beam parameters for the higher-brightness HL-LHC beams is complex. Assuming, for example, that similar fractions of the total stored beam energies were located in the beam halo, the stored beam energy above $3\sigma_N$ would yield 35 MJ. This is enough to damage the LHC collimators in case of sudden orbit shifts, for example, in case of crab-cavity failure [6]. Therefore, measures are needed to mitigate this peril.

Hollow electron lenses (HEL) [7] for active halo removal are considered to be deployed in HL-LHC, but cannot be manufactured in time for Run 4 operation. Understanding the formation and population of the halo in LHC Run 3, the final run before HL-LHC installation, is therefore a critical task. The main goals of these activities are reviewing the expected risk from the halo population in HL-LHC, exploring alternative mitigation strategies, and defining requirements for monitoring the halo in HL-LHC.

In this article, we review the technique used for halo quantification in the LHC and discuss data recorded in LHC Run 2 to compare against measurements performed in Run 3. We will then outline the merits of additional measurements planned for in LHC Run 3 and close the article with an outlook on the challenges of halo quantification for HL-LHC.

COLLIMATOR SCANS FOR HALO MEASUREMENTS

LHC collimators are equipped with one or two movable jaws of a robust material used to scatter and/or absorb beam particles. Different collimator types are used, following a defined hierarchy [8]. Primary collimators (TCP) are the only LHC components designed to be directly exposed to the main beam. They are built with two 60 cm long jaws made of a low-density material [9]. This assures robustness against high loads of particle fluxes while providing scattering toward larger amplitudes, where the particles can be intercepted by the secondary collimators and their shower absorbers. Each jaw can be moved independently by two stepper motors, with a step size of $5\mu\text{m}$ [10].

Each collimator is equipped with a beam loss monitor (BLM) [11] downstream, as illustrated in Fig. 1. BLMs are ionisation chambers, measuring local secondary particle showers created when particles leave the beam vacuum and interact with surrounding matter. More than 3000 BLMs

* Work supported by the HL-LHC project.

[†] pascal.hermes@cern.ch

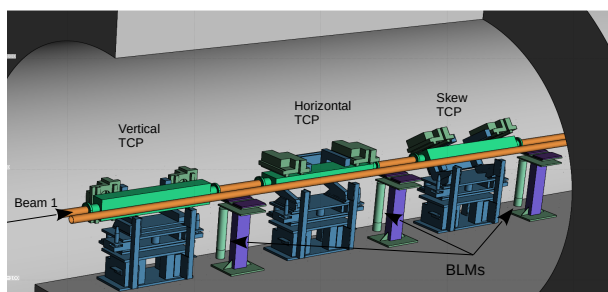


Figure 1: 3D model of LHC Beam 1 primary collimators (TCPs) in the LHC tunnel. The BLMs downstream of each collimator are clearly visible. Image source: Ref. [12].

are installed in the LHC, allowing for global monitoring of particle losses over twelve different integration times from 40 μ s to 84 s [11]. They are part of the LHC beam interlock system: a beam dump is triggered if signals recorded in the LHC BLMs exceed predefined thresholds [13]. Furthermore, diamond-BLMs (dBLMs) are installed downstream of the primary collimators, providing a time resolution in the ns range to identify bunch-by-bunch losses [14].

Halo Measurement Technique

Halo measurements are based on beam scraping with the collimator jaws by moving one or both TCP jaws towards the beam centre in steps, thus reducing the applied betatron cut in the horizontal (H) or vertical (V) plane. This is done after a beam-based alignment of the jaws to ensure that the centre of the beam at the collimator is accurately known [15]. The precise knowledge of the collimator jaw positions allows computing the cut in beam σ_N units. The starting point of the scan is typically the nominal collimator position of $5 \sigma_N$ for LHC Run 2 and Run 3 at top energy. All collimators, except the TCP, remain in their nominal positions. Halo measurements are usually performed with the highest stored beam energies, which is representative of nominal high-intensity physics operation as effects such as impedance, Landau octupoles, beam-beam, e -cloud, etc. are nominal. The highest stored beam energy during a measurement in 2022 was roughly 200 MJ.

Consider Fig. 2, where measured data is shown for a measurement performed in 2022. The collimator betatron cut is shown as a black line. The individual collimator steps of 5 μ m step size are clearly visible. The loss of beam particles is visible as spiking in the collimator BLM signal (orange line) when the jaw is moved. The red line shows the number of particles lost since the beginning of the scraping, measured with the direct current LHC Beam Current Transformer (BCTDC) [16]. In the example shown, roughly 1.6×10^{11} charges were lost during the scraping to a betatron cut of $3 \sigma_N$, roughly 0.7% of the initial beam intensity.

Considering each collimator step, a clear change of the BCT signal is not measurable for the small loss amounts when scraping at large betatron amplitudes. With the noise level and sensitivity of the BCTDC, a clear intensity drop is

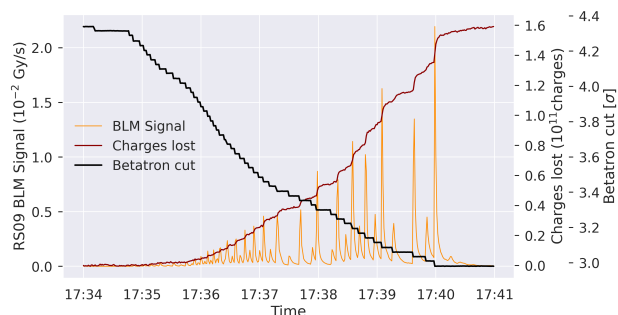


Figure 2: Data recorded during a vertical scraping of LHC Beam 2 (B2V). The black line shows the betatron cut applied. The red line reflects the cumulative amount of charges lost, measured with the BCTDC (initial total beam intensity of 2.38×10^{13} charges). The orange line represents the BLM signal at the collimator with 1.3 s integration time.

visible if it exceeds a value of the order of 10^9 charges. A similar boundary is observed for the total intensity derived from the bunch-by-bunch measurement with the fast BCT (BCTFR) [16].

The BLM signal shows clear spikes already at larger betatron amplitudes with lower halo densities. The BLMs can therefore be used to identify smaller amounts of lost particles, thanks to their higher sensitivity and a large dynamic range of more than 10^8 (10 pA–1 mA). For the BLMs at the primary collimators, beam losses of the order of 5×10^4 charges to 5×10^{12} charges could be detected.

BCT-based Post Processing

Based on the change in beam intensity recorded with BCTFR or BCTDC at each collimator step, the cumulative halo content can be derived. The total fraction of the beam intensity stored above a given amplitude is directly deduced from the fraction of the initial intensity lost until a given betatron cut is reached. The limited sensitivity for small loss amounts discussed before imposes a lower limit for the halo that can still be quantified. This is visible in the comparison of the reconstructed halo population using the BCTDC and the BLM system (see next section) shown in Fig. 3. We used the minimum and maximum of the BCTDC signal, while a given collimator setting was applied, to quantify the uncertainty.

Using the BCTFR signal, it is possible to disentangle the lost intensity for each circulating bunch. Analyses of the latter unveiled considerable differences in the bunch-by-bunch halo population. It is also noteworthy that the BCTFR signal is logged for longitudinally confined beam particles, while the BCTDC signal also records de-bunched beam intensity.

BLM-based Post Processing

A calibration model can be applied to a subset of BLM signals, measured in Gy/s, to estimate the number of charges lost per collimator step [17]. This allows us to benefit from their larger dynamic range, which is especially useful in

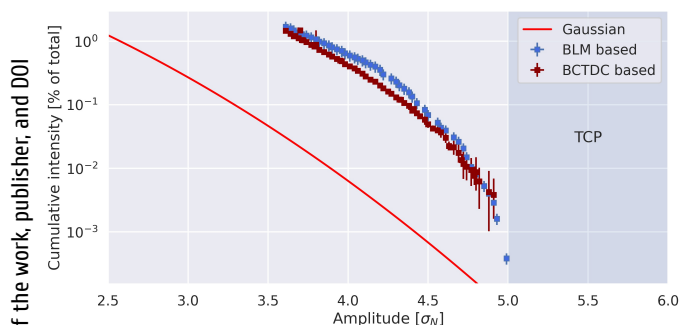


Figure 3: Example of halo population vs. amplitude, derived from a halo scraping measurement in 2022. The halo population derived from BCTDC data is marked in red, from BLM data in blue. The Gaussian is given for reference and refers to the nominal emittance of $3.5 \mu\text{m rad}$.

regions with low particle densities. The calibration is based on the response of the BLM signal to beam losses in the different TCPs, measured during collimation qualification loss maps [18]. These are machine-protection validation tests during which well-defined beam loss scenarios are reproduced independently by exciting the beams horizontally or vertically with white noise. The response of the BLM signal to each beam loss scenario is then calculated as the accumulated BLM signal divided by the total lost intensity measured by the BCT.

The BLMs with high and similar signal responses to the loss scenarios involving one of the beams and low signal responses for the other beam are selected and a combined signal response to beam impacts on the TCPs is calculated. The lost charges are then calculated by multiplying this signal response by the sum of the selected BLMs signals. The uncertainty in the measurements is given by considering the noise in the BCTs and BLMs signals both during the loss maps and the beam scraping periods. This calibration is especially useful to disentangle beam losses due to luminosity burn-off and from collimation cleaning.

The blue graph in Fig. 3 shows the relative fraction of total beam intensity lost throughout a scraping to $3 \sigma_N$, estimated based on the BLM calibration obtained in 2022.

Conclusions

The BLM- and BCT-based analysis deliver similar results for the halo population. For large amplitudes, with low beam densities, the intensity drop is below the noise level and the BCT measurement is not usable. Thus, especially when measurements at larger betatron amplitudes are carried out, the BLM-based analysis becomes the method of choice.

MEASUREMENT RESULTS

LHC Run 2

The measurements carried out in LHC Run 2 are described in detail in Ref. [4]. Here, we review the main findings in Ref. [4] and provide additional information for the measure-

ment in which the highest halo population was found (fill 6194).

Eleven measurements were carried out, two of which with nominal optics, and the rest with so-called ATS optics [19]. All measurements, except one, were performed with colliding beams at the smallest β^* applied (in LHC IP1 and IP5) in the given year: 40 cm in 2016 (nominal optics) and 2017 (ATS), and 25 cm in 2018 (ATS). One measurement was performed with separated beams, in the “flat-top” stage of the 2018 LHC cycle with $\beta^* = 1 \text{ m}$.

A summary of the maximum lost beam intensity K for a subset of the measurements, taken from Ref. [4], is shown in Fig. 4. It is based on a simple BLM calibration, using only one BLM. A clear pattern across the measurements cannot be identified, and a direct comparison is not possible due to the different minimum betatron cut P_{\min} (in nominal beam size) reached in the different measurements. Also, the beam emittances were different in each fill.

A maximum value of K of almost 5 % of the total stored beam energy is reached in the B2V plane for an amplitude greater than $3.1 \sigma_N$ in fill 6194. Two more planes (B1H/B1V) show a population greater than 4 %. However, this fill was exceptional in different ways: the bunch intensities were of 1.3×10^{11} particles per bunch (ppb), compared to 1.15×10^{11} ppb in the other measurements. The emittances measured with the wire scans [20] at injection were highest during fill 6194: between $2.6 \mu\text{m rad}$ and $2.8 \mu\text{m rad}$, compared to $1.7 \mu\text{m rad}$ to $2.5 \mu\text{m rad}$ for all other measurements (we assumed a 20 % emittance increase during the energy ramp [21]). The larger beam size in this fill partially explains the higher halo population. The scraping was done in an environment of strong non-linearities: The octupoles were operated at their maximum currents of 570 A, compared only with 340 A to 400 A in the other fills. The combination of the high halo population observed could be explained by a non-linear deformation of the phase space. The collimator position measured in linear beam σ_N would then reflect a different, smaller, betatron cut than expected.

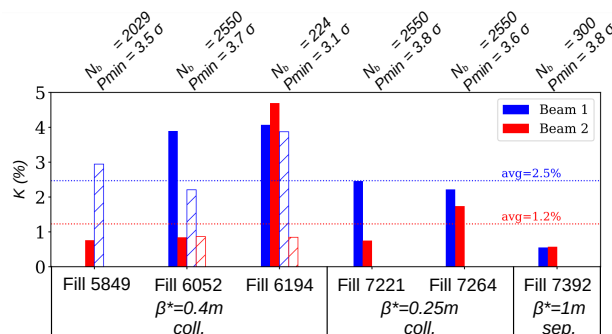


Figure 4: Halo content, K , for selected Run 2 measurements. N_b refers to the number of bunches, P_{\min} to the minimum betatron cut achieved with the primary collimator. Hatched/solid bars: H/V plane. All measurements were done with ATS optics. Figure adapted from Ref. [4].

It is foreseen to study this hypothesis further in dedicated particle-tracking simulations including beam-beam effects.

For Fill 7392, the measurement after the energy ramp and before colliding the beams shows a comparably low halo population of less than 0.5 %. We interpret this finding as an indication that the relevant halo formation process could be induced by collisions.

LHC Run 3

Three halo population measurements were performed in 2022 after several hours of collisions in regular physics fills, at the end of the luminosity levelling [22] with $\beta^* = 30$ cm. After each scraping a dedicated sequence of collimator settings was applied to measure non-linear diffusion coefficients [23]. The first two measurements were made with the primary purpose of gathering data for BLM calibration, for which it was necessary to separate the colliding beams. The last scraping was fully dedicated to halo quantification and diffusion studies, and the beams were kept in collision.

The halo contents derived from the measurements are summarised in Fig. 5. The halo content observed is below those measured in Run 2. The maximum is reached with 1.3 % of the total stored beam intensity above $3.5 \sigma_N$ in the B1H plane during fill 8387 with a bunch intensity of 1.44×10^{11} p. Note that the beams injected into the LHC in Run 3 were produced after full deployment of the LIU project with an improved brilliance compared to Run 2. In this fill, emittances of up to $2 \mu\text{m rad}$ were measured.

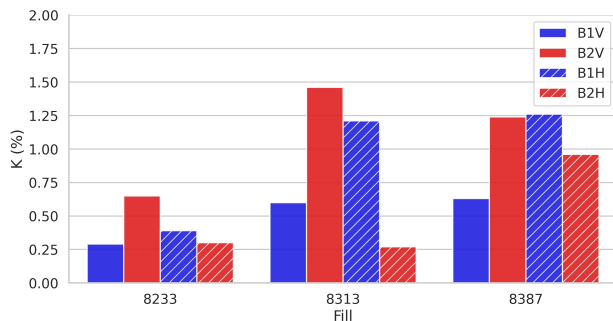


Figure 5: Fraction of beam intensity lost per scraping, K , for selected Run 3 measurements. Hatched/solid bars: H/V plane. Note the different scale compared to Fig. 4.

PLANS FOR THE REMAINDER OF RUN 3

The formation and magnitude of the beam halo are not well understood. We intend to carry out a series of measurements for the remainder of LHC Run 3 to gain a more tangible understanding of the halo population throughout the LHC cycle, with beam properties as closely as possible to the HL-LHC parameters. Measurements in the final stage of luminosity levelling will be repeated with bunch intensities approaching the Run 4 intensities of at least 1.7×10^{11} ppb [24].

Measurements at the injection stage are planned to understand the correlation of the LHC halo population to scrapings

in the CERN Super Proton Synchrotron (SPS), the LHC's injector. The insights will help determine the potential of reducing the halo content at injection. These measurements are planned to be enhanced by wire-scan measurements with different gains of the shower detector to create sensitivity to the lower signal at the halo.

All measurements carried out so far were made by serial scraping of the horizontal and vertical planes with the same beam. This could introduce a bias for the plane that is scraped secondly. We intend to study this at injection energy by scraping one bunch train in plane H and injecting another bunch train without dumping the previous one to scrape both in the V plane. The latter shall then be combined with a subsequent energy ramp of the two scraped trains and one unaltered train. This will allow to identify the halo repopulation during the ramp and quantify the halo population after the energy ramp, before bringing the beams into collision.

OUTLOOK TOWARDS HL-LHC

As introduced before, the beam halo could pose a serious threat to HL-LHC operational safety and/or efficiency. Scraping measurements will remain an important method also in the HL-LHC era. However, having means of active and non-destructive halo monitoring for interlocking becomes crucial. The requirement of being nondisruptive to the circulating beam led to the consideration of synchrotron radiation as a sensible carrier of information. A synchrotron light-based coronagraph [3] was designed for the LHC and testing of the device is ongoing during LHC Run 3. This device must be capable of accurately identifying halo populations at amplitudes between $3.6 \sigma_N$ and $8.5 \sigma_N$, to cover all relevant operational scenarios [24]. Note that for HL-LHC, σ_N corresponds to a reference normalised transverse emittance of $2.5 \mu\text{m rad}$. An interlock strategy could be based on the integrated stored beam energy within a given distance from the TCPs, in two dimensions. Sudden orbit shifts of up to $2 \sigma_N$ should be tolerated. Therefore, a beam dump should be triggered if the halo content within $N_p - 2 \sigma_N$ exceeds a certain threshold, where N_p is the half-gap of the primary collimator. Possible means of active halo depletion without HELs are currently under study.

CONCLUSION

The large population of transverse beam halos could pose a serious threat to HL-LHC. We discussed the technique of collimator scans to quantify transverse beam halos in the LHC, based either on BCT measurements or calibrated BLM signals. Both provide similar results, but the BLM method is also sensitive to lower loss levels and is the only method available for large amplitudes with low beam intensities. The Run 2 and Run 3 scraping data show a large variability of the recorded halo populations that is not fully understood. More measurements during LHC Run 3 are needed to understand the halo population and formation in HL-LHC. Halo monitoring and interlocking strategies in HL-LHC must be developed to ensure machine safety at any time.

REFERENCES

- [1] O. S. Brüning *et al.*, “LHC Design Report,” Tech. Rep., 2004. doi:10.5170/CERN-2004-003-V-1
- [2] R. Bruce *et al.*, “Simulations and measurements of beam loss patterns at the CERN Large Hadron Collider,” *Phys. Rev. ST Accel. Beams*, vol. 17, no. 8, p. 081004, 2014. doi:10.1103/PhysRevSTAB.17.081004
- [3] A. Goldblatt, E. Bravin, F. Roncarolo, G. Trad, and T. M. Mitsuhashi, “Design and Performance of Coronagraph for Beam Halo Measurements in the LHC,” in *Proc. IBIC'16*, Barcelona, Spain, Sep. 2016, pp. 253–256. doi:10.18429/JACoW-IBIC2016-MOPG74
- [4] A. Gorzawski *et al.*, “Probing LHC halo dynamics using collimator loss rates at 6.5 TeV,” *Phys. Rev. ST Accel. Beams*, vol. 23, p. 044802, 2020.
- [5] O. Aberle *et al.*, *High-Luminosity Large Hadron Collider (HL-LHC): Technical Design Report*. CERN, Geneva, Switzerland, 2020. doi:10.23731/CYRM-2020-0010
- [6] A. Santamaria Garcia, “Experiment and Machine Protection from Fast Losses caused by Crab Cavities in the High Luminosity LHC,” Doctoral Thesis, 2018. doi:10.5075/epfl-thesis-8533
- [7] S. Redaelli *et al.*, “Hollow electron lenses for beam collimation at the High-Luminosity Large Hadron Collider (HL-LHC),” *J. Instrum.*, vol. 16, no. 03, P03042, 2021. doi:10.1088/1748-0221/16/03/p03042
- [8] R. Bruce, R. Assmann, L. Lari, and S. Redaelli, “Collimator hierarchy limits: assumptions and impact on machine protection and performance,” *MPP Workshop March 2013, Annecy, France*, 2013.
- [9] C. Accettura *et al.*, “Overview of material choices for HL-LHC collimators,” presented at IPAC'23, Venice, Italy, May 2023, paper WEPA148.
- [10] S. Redaelli, R. W. Assmann, R. Losito, and A. Masi, “Final Implementation and Performance of the LHC Collimator Control System,” in *Proc. PAC'09*, Vancouver, Canada, May 2009, pp. 4788–4790.
- [11] B. Dehning *et al.*, “The LHC Beam Loss Measurement System,” 2007, LHC-PROJECT-Report-1025, CERN-LHC-PROJECT-Report-1025.
- [12] E. Skordis *et al.*, *Updates on FLUKA simulations of the 4 TeV quench test*, Presentation in the LHC Collimation Working Group 181, 2014.
- [13] B. Puccio, A. Castañeda, M. Kwiatkowski, I. Romera, and B. Todd, “The CERN Beam Interlock System: Principle and Operational Experience,” in *Proc. IPAC'10*, Kyoto, Japan, May 2010, pp. 2866–2868.
- [14] E. C. Giraldo *et al.*, “The Diamond Beam Loss Monitoring System at CERN LHC and SPS,” in *Proc. IBIC'22*, Kraków, Poland, 2022, pp. 202–206. doi:10.18429/JACoW-IBIC2022-TU2C2
- [15] G. Valentino *et al.*, “Comparison of LHC Collimator Beam-Based Alignment Centers to BPM-Interpolated Centers,” in *Proc. IPAC'12*, New Orleans, LA, USA, May 2012, pp. 2062–2064.
- [16] D. Belohrad, L. K. Jensen, O. R. Jones, M. Ludwig, and J. J. Savioz, “The LHC Fast BCT system: A comparison of Design Parameters with Initial Performance,” CERN, Tech. Rep., 2010, CERN-BE-2010-010.
- [17] S. M. Vigo *et al.*, “Beam lifetime monitoring using beam loss monitors during LHC Run 3,” presented at IPAC'23, Venice, Italy, May 2023, paper THPL086.
- [18] V. Moens, R. Bruce, S. Redaelli, B. Salvachua, and G. Valentino, “Comparison of LHC Beam Loss Maps using the Transverse Damper Blow up and Tune Resonance Crossing Methods,” in *Proc. IPAC'13*, Shanghai, China, May 2013, pp. 1008–1010.
- [19] S. Fartoukh, “Achromatic telescopic squeezing scheme and application to the LHC and its luminosity upgrade,” *Phys. Rev. ST Accel. Beams*, vol. 16, no. 11, p. 111002, 2013. doi:10.1103/PhysRevSTAB.16.111002
- [20] J. Bossier and C. Bovet, “Wire Scanners For LHC,” CERN, Tech. Rep., 1997, LHC-Project-Note-108.
- [21] S. Papadopoulou *et al.*, “Monitoring and Modelling of the LHC Emittance and Luminosity Evolution in 2018,” in *Proc. IPAC'19*, Melbourne, Australia, May 2019, pp. 3212–3215. doi:10.18429/JACoW-IPAC2019-WEPTS046
- [22] S. Fartoukh *et al.*, “LHC Configuration and Operational Scenario for Run 3,” CERN, Tech. Rep., 2021, CERN-ACC-2021-0007.
- [23] C. E. Montanari, A. Bazzani, M. Giovannozzi, P. Hermes, and S. Redaelli, “Recent measurements and analyses of the beam-halo dynamics at the CERN LHC using collimator scans,” presented at IPAC'23, Venice, Italy, May 2023, paper WEPA022.
- [24] R. Tomas Garcia *et al.*, “HL-LHC Run 4 proton operational scenario,” CERN, Tech. Rep., 2022, CERN-ACC-2022-0001.